SHORELINE SAND WAVES ALONG THE CATALAN COAST

A. Falqués[1], M. Caballeria[2], F. Ribas[1] and N. van den Berg[1]

Abstract

The beach of Calella, north of Barcelona, in the Catalan coast, features a series of shoreline sand waves with wavelengths ranging from 700 to 1400 m that match with similar undulations in the -5 m bathymetric line. Historical satellite images from 2002 till 2010 show that these undulations slightly change in time. The wave climate on that stretch of the Catalan coast has a large proportion of waves from the E-NE and from the SW, i.e., with high angles with respect to shore normal rending the shoreline potentially unstable. Here we show that those sand waves might be due to that instability. Model results, both Linear Stability Analysis and nonlinear time evolution, show that the shoreline is nearly at the threshold for instability and that the emergent wavelengths are roughly consistent with the observed ones.

Key words: shoreline sand waves, shoreline instability, high angle waves, alongshore sediment transport, wave climate, Catalan coast

1. Introduction

Shoreline sand waves are undulations of the shoreline that extend into the bathymetry up to a certain depth. Some of them are linked to surfzone rhythmic bars (megacusps) but we will here focus on those that are not necessarily linked to surfzone bars and that in general occur at larger length and time scales, i.e., km's and yr's. These shoreline sand waves are episodically or persistently found along many sandy coasts (Bruun 1954, Verhagen, 1989, Inman et al. 1992, Thevenot and Kraus 1995, Gravens 1999, Stive et al. 2002, Ruessink and Jeuken 2002, Davidson-Arnott and van Heyningen 2003, Medellín et al. 2008, Falqués et al. 2011a, Kaergaard et al. 2011, Ryabchuk et al. 2011). Sometimes they are clearly visible at naked-eye (e.g., Falqués et al. 2011a, Ryabchuk et al. 2011) but they can also be very subtle, being visible only from long term shoreline evolution after removing the trend (Ruessink and Jeuken, 2002). They can be triggered by different physical mechanisms, including forcing by offshore bathymetric anomalies or input of large quantities of sand at inlets and rivers, but they can also emerge from irregularities of an otherwise rectilinear coast in absence of any forcing at their length scale. This can occur if the wave climate is dominated by high-angle waves, i.e., waves with a high incidence angle relative to the shore normal, because the rectilinear coast becomes unstable (Ashton et al. 2001, Ashton et al. 2006a, Falqués et al. 2011b) and we will hereinafter refer to them as free or self-organized sand waves. The critical water wave angle for instability is about 45^o at the depth of closure, i.e., at the most offshore reach of the bathymetric perturbations (van den Berg et al. 2012).

The Catalan coast is located at north-eastern Spain, at the western side of the Mediterranean Sea, and extends from the border between France and Spain in the north (42.5°N; 3.25°E), until Ebro delta in the south (40.5°N; 0.5°E). The wave climate is quite bimodal, with a large proportion of events with high angle waves from east-northeast and from south-southwest. This coast is therefore potentially unstable and its sandy beaches could perhaps develop shoreline sand waves. However, the Catalan coast has important rocky stretches and has many urbanized areas with harbours and groins with the result that there is a lack of long uninterrupted sandy beaches. The typical wavelengths of free shoreline sand waves are in the range of 1-10 km and it is hard to find uninterrupted sandy beaches of this length or longer. Therefore, even if the wave climate could be prone to generate free shoreline sand waves, perhaps the beaches are not long

[1]Departament de Física Aplicada, Universitat Politècnica de Catalunya, Barcelona, Catalonia, Spain. albert.falques@upc.edu

[2] Escola Politècnica Superior, Universitat de Vic, Vic, Catalonia, Spain. miquel.caballeria@uvic.cat

enough to allow for such instability. And indeed, such sand waves are not self-evident at naked-eye along most of the Catalan coast (perhaps an analysis of principal components of coastline variability could reveal shoreline undulations governed by high-angle wave instability). One exception is the coast of El Maresme, from Barcelona to Blanes, just south of the rocky Costa Brava. The northern part of this coast, near Calella town, is a 6 km uninterrupted sandy beach that features a train of sand waves with 4 salients (see image from Google Earth, 31/12/2006). The spacing from crest to crest ranges from 700 to 1400 m (Figure 1).

The aim of this contribution is to test whether the wave conditions at El Maresme coast together with the cross-shore beach profile lead to coastline instability and in such a case which is the dominant wavelength and the growth rate. In particular, we want to test the hypothesis that the undulations of the shoreline near Calella are governed by shoreline instability due to high angle waves.

2. Morphology and wave climate of El Maresme coast

2.1. *Coastal morphology and shoreline sand waves*

We consider the 6 km sandy beach coast north of Calella light house (Figure 1). This is a coarse sand beach ($D_{50}\approx$ 1.4 mm) with a steep slope at the swash zone ($\beta \approx 0.07$) and a mean distance of Δx=700 m. from the D= -10.4 m bathymetric line to shore. The angle of the mean shoreline with the North is 70^o. A series of subtle undulations occur along this beach (Figure 1) with an amplitude up to about 50 m (cross-shore displacement of the crests from the embayments) and a spacing ranging from 700 m to 1400 m. Historical images from Google Earth indicate that the sand waves have slightly changed during the period 2002-10., being quite visible during 2002-2009 and less visible during 2010. Figure 2 shows that similar undulations exists too in the D=-5m bathymetric line in a stretch of coast of 13 km that includes Calella beach at its northern part (yellow line). By considering that in the bathymetric contour line there are 10 undulations, the mean wavelength is about $\lambda \approx 1300$ m and the mean amplitude is $a \approx 130$ m. The undulations of the

Figure 1. Left: Catalan coast in the white rectangle and El Maresme coast in the yellow rectangle. Right: Calella beach featuring shoreline sand waves with 4 crests and 5 embayments. From Google Earth.

bathymetric contour line are clearly correlated to the shoreline undulations at Calella beach. This can be seen in Figure 2, where the salients and the maximum offshore shifts at the bathymetric contour are indicated by red circles. The correspondence between the onshore shifts in both lines is quite evident.

In order to perform linear stability analysis with 1D-morfo model, the slope of the beach profile at the shoreline, and the unperturbed cross-shore profile, $D_0(x)$, (at least from the shore to the offshore boundary) are required. The offshore boundary has been placed at 90 m depth, so that wave conditions at Palamós and Tordera delta buoys can be taken as a representative for all the area. Two cross-shore sections S_1 and S_2, one at a salient and the other at an embayment have been considered (they are indicated by the dashed lines in Figure 3).

2.2. *Wave climate*

The wave climate (Figure 4) has been taken from Blanes buoy, which is located at 41^o 38.81' N, 2^o 48.93' E, in 74 m depth. It is to the E-NE from Calella beach at a distance of about 5 km. It is seen that the waves from E-NE are dominant in the sense that they are more frequent and higher. Also their periods are greater

than the period of SW waves.

Figure 2. Satellite image from Google Erath of the coastline of El Maresme that extends from Arenys de Mar harbour to Tordera river delta. The superposed yellow line (13 km alongshore length) corresponds to the bathymetric contour line of 5 m depth that has been obtained from the Sistema d'Informació Geografica del Litoral de Catalunya SIGPesca. Calella beach is nearly at the center of the coastline that is shown. The red dots indicate the salients in the shoreline and the most offshore position of the bathymetric contour line in front of Calella.

Figure 3. Plan view of the beach of Calella. Red circles indicate two consecutive salients along Calella beach with a spacing of 1240 m. The cross-shsore displacement of the tip of the salients with respect to the embayments (amplitude) is $a_s \approx 48$ m.

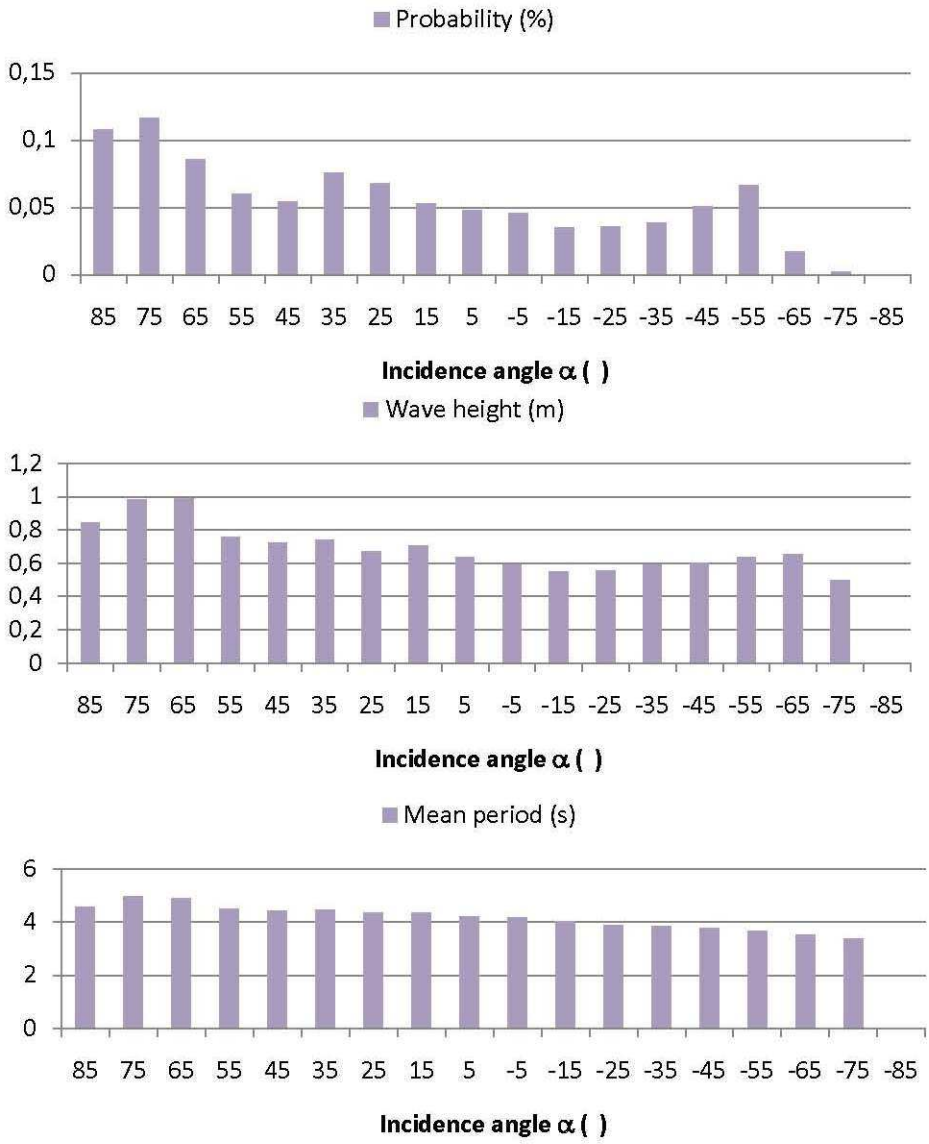

es are with
g from E.

3. Long term coastline models

3.1. *Linear stability model*

A linear stability model developed by the research team (1D-morfo model) is used to explore the potential shoreline instability along the Catalan coast. A very brief description of this model is given here and the reader is referred to Falqués and Calvete (2005) for further details. The model describes the dynamics of small amplitude perturbations of an otherwise rectilinear coastline. Following the one-line concept, the dynamics is governed by the gradients in the total alongshore wave-driven transport rate Q:

$$D_a \frac{\partial x_s}{\partial t} = -\frac{\partial Q}{\partial y} \tag{1}$$

A Cartesian coordinate system is assumed, x seawards in the unperturbed cross-shore direction and y running alongshore. The position of the shoreline is given by $x = x_s(y, t)$, t is time and D_a is the active water depth which is of the order of the depth of closure. This active water depth is directly related with the one-line concept (for more details, see Falqués and Calvete, 2005). The transport rate Q is computed according to the alongshore sediment transport formula of the CERC (USACE, 1984)

$$Q = \mu H_b^{5/2} \sin(2(\theta_b - \phi)) \tag{2}$$

where H_b is the root mean square wave height at breaking, θ_b is the angle between wave fronts and unperturbed coastline at breaking, $\phi = \tan^{-1}(\partial x_s / \partial y)$ gives the local orientation of the perturbed shoreline and β is the beach slope at the instantaneous shoreline (i.e. the waterline). The constant μ is proportional to the empirical parameter K of the original CERC formula and is of order $0.1-0.2$ m$^{1/2}$ s^{-1}. Unless stated otherwise, a value $\mu = 0.15$ m$^{1/2}$ s^{-1} is chosen for this contribution, which corresponds to $K = 0.53$.

To compute the sediment transport rate according to eqn. (2), $H_b(y, t)$ and $\theta_b(y, t)$ are needed. The procedure to determine them is as follows. It is assumed that the wave height and wave angle are alongshore uniform in deep water. Then, wave transformation including refraction and shoaling is performed from deep water up to breaking so that $H_b(y, t)$ and $\theta_b(y, t)$ are determined and Q can be computed. To do wave transformation, a perturbed nearshore bathymetry coupled to the shoreline changes is assumed:

$$D(x, y, t) = D_0(x) - \beta\, f(x)\, x_s(y, t) \tag{3}$$

where $D(x, y, t)$ and $D_0(x)$ are the perturbed and unperturbed water depth, respectively, and $f(x)$ is a shape function that, at the shore, $x = 0$, takes the value $f(0) = 1$ in order to shift the shoreline to the perturbed position $x = x_s(y, t)$. For the present work, it has been taken

$$f(x) = \frac{e^{-x/L} - e^{-x_c/L}}{1 - e^{-x_c/L}} \qquad 0 \le x \le x_c \tag{4}$$

where x_c is the cross-shore distance from the shore to the location of the depth of closure, $D_0(x_c) = D_c$, and L is the "characteristic" length of the bathymetric perturbation, which is a free parameter of the model. Beyond the depth of closure, $x > x_c$, the perturbation vanishes and $f(x) = 0$ has been taken. It was shown (Falqués and Calvete, 2005) that a crucial factor for shoreline instability is the coupling between the surf and the shoaling zones, which is accomplished only if L is large enough, at least a couple of times the surf zone width. This parameter can be seen as a way to parameterise the cross-shore sediment exchange, especially between the surf and shoaling zones. This makes this instability essentially different from the surf zone morphodynamic instabilities leading to rhythmic bars and rip channels. The changes in the shoreline cause changes in the bathymetry (both in the surf and shoaling zones) which in turn cause changes in the wave field. The changes in the wave field affect the sediment transport that drives shoreline evolution. Therefore, the shoreline, the bathymetry and the wave field are fully coupled.

Following the linear stability concept, the perturbation of the shoreline is assumed to be

$$x_s(y, t) = a\, e^{\sigma t + iky} + c.c.$$

where a is a small amplitude. For each given (real) wavenumber, k, this expression is inserted into the governing equation, eqn. (1), and into the perturbed bathymetry, eqn. (3). By computing the perturbed wave field and inserting H_b and θ_b in eqn. (1), the complex growth rate, $\sigma(k) = \sigma_r + i\sigma_i$, comes out. All the equations are linearized with respect to the amplitude, a. Then, for those k such that $\sigma_r(k) > 0$, a sandwave with wavelength $\lambda = 2\pi/k$ tends to emerge from a positive feedback between the morphology and the wave field. The pattern that has the maximum growth rate is called the Linearly Most Amplified mode (LMA mode) and it is the one which should be comparable to observations. The model has been applied to the sandwaves along the Dutch coast (Falqués, 2006) and to the sandwaves along El Puntal beach - Spain (Medellín et al., 2009).

3.2. *Quasi 2DH model*

The Linear Stability Model gives just the tendency to grow or decay of the perturbations. To describe the time evolution of the perturbations and the dynamics of the sand waves up to certain amplitude a nonlinear model has been built (Q2D-morfo). This model does not use linear approximations of the equations and in addition, the assumption of an instantaneous reaction of the bathymetry to shoreline changes or vice versa is removed. This is done by considering a parameterization of cross-shore sediment transport. To this aim, a 2D horizontal domain including dry beach and submerged beach is considered with a bed level given by $z_b(x,y,t)$ (coordinate system like in section 3.1). The coastline, $x = x_s(y, t)$, is the boundary between the grid cells with $z_b(x,y,t)>0$ and those with $z_b(x,y,t)<0$. The sediment conservation in one dimension, eq. (1), is substituted by the sediment conservation in 2D:

$$\frac{\partial z_b}{\partial t} + \frac{\partial q_x}{\partial x} + \frac{\partial q_y}{\partial y} = 0 \qquad (5)$$

where (q_x,q_y) is the depth integrated sediment flux. This flux is computed directly from the waves at breaking in a parameterized way. It consists of an alongshore component that is a cross-distribution of the total transport rate given by eq. (2) plus a cross-shore component that is proportional to the difference between the actual bed slope and certain equilibrium bed slope. This essentially describes the alongshore transport given by the CERC formula, eq. (2), and the tendency of the cross-shore profile to gradually adapt to an equilibrium profile. The wave field is given at the offshore boundary and is computed in the domain by using the wave rays approximation over the changing bathymetry. Regarding the horizontal grid, sediment conservation and morphological updating the model is like a 2DH model. The difference is that the nearshore hydrodynamics is not explicitly resolved because the sediment transport is computed directly from the waves. This makes the model capable of long time runs (years) in large domains (alongshore lengths of tens of km). The model is initialized with either a localized bump in an otherwise rectilinear coastline or with small random perturbations of otherwise rectilinear bathymetric lines. Then both the bathymetry (and shoreline) and the wave field evolve in time in a fully coupled way. This is just a sketch of the model; a detailed description can be seen in van den Berg et al. (2012).

4. Tests with constant wave conditions

4.1 *1D-morfo model*

A necessary test is to check whether for high angle waves, i.e., removing all the low angle waves from the wave climate, there is instability and with what dominant wavelength and growthrate. If the wavelength was very different from the observed one or if the growthrate was very low, going on with the study would be pointless. We selected the basic beach profile of section S2 (Figure 3) and we considered constant wave conditions representative of mean conditions from waves coming from E-NE or from SW. Consistently with the wave climate we selected a number of wave periods, T=4, 5, 6 s, and we then made a sensitivity analysis for the wave angle and the wave height. Figure 5 shows typical results that have been obtained for T=5 s. According to the wave climate, the relevant mean Hs in case of E-NE waves should be in the range 0.8-1 m. In this case, the maximum instability is found for $\theta \approx 70^o$ with a wavelength of $\lambda \approx$ 1-1.1 km and a characteristic growth time, $\sigma^{-1} \approx$ 0.7-1 yr. For T=6 s (not shown) the instability would be weaker, $\sigma^{-1} \approx$ 1-2 yr and longer wavelengths $\lambda \approx$ 1.1-1.4 km. Therefore, we conclude that Calella beach with only waves coming from E-NE would be unstable and would develop sand waves of roughly the observed wavelength.

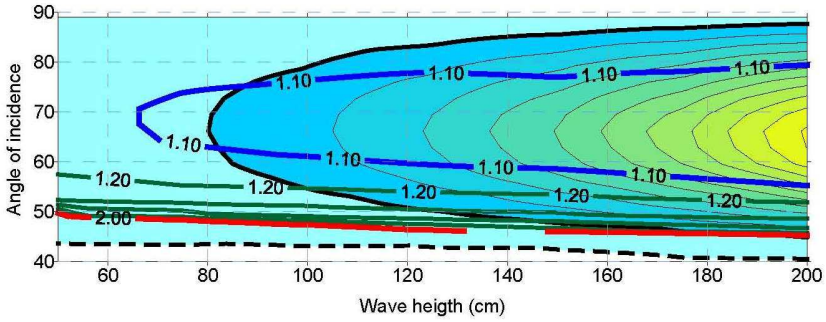

Figure 5. Linear stability analysis for constant wave conditions. The contour lines of real growthrate, σ, are shown as a function of wave height (Hs) and incidence angle with respect to shore normal. The dashed line indicates neutral stability, σ=0. The thick black solid line indicates σ=1 yr^{-1}. The thinner black solid lines and the colors from blue to yelow indicate growthrates faster than σ=1 yr^{-1}. The blue thick line indicates the dominant wavelength of λ = 1.1 km.

4.2 *Q2D-morfo model*

Three more tests have been conducted for constant wave conditions, now with Q2D-morfo. A rectangular domain of 10 km alongshore and 0.8 km cross-shore (including a dry beach of 100 m width) has been considered. The shoreline is initially rectilinear except for a smooth bump of 24 m amplitude and either 0.5 or 1 km width. The wave conditions for test #1 have been selected by taking an average of all the waves from E-NE in the wave climate. Similarly test #2 corresponds to the average of all waves coming from SW. Test #3 is for constant wave conditions corresponding to the peak of an E-NE storm. In all the tests with Q2D-morfo, the value $\mu = 0.2\ m^{1/2}\ s^{-1}$ is used, which corresponds to K = 0.7.

Table 1. Tests with Q2D-morfo. The angle is with respect to shore normal (positive from the SW)

Test #	waves: Blanes buoy			waves: offshore boundary		
	θ	H_s (m)	T_m (s)	θ	H_s (m)	T_m (s)
1	-70	0.82	4.7	-66	0.71	4.7
2	63	0.42	3.9	62	0.41	3.9
3	-75	2.6	7.8	-46	1.47	7.8
4	actual wave climate (see table 2)					

Consistently with the Linear Stability model, tests 1 and 2 cause instability. The initial bump is damped and widened and a series of shoreline undulations develop downdrift of it starting with a very pronounced embayment. At the same time, the growing undulations migrate downdrift. The instability is slightly stronger for SW waves than for E-NE waves (Figure 6). The wavelength ranges from 600 to 800 m being slightly shorter for SW waves. Interestingly, the E-NE storms, which are the dominant storms in the wave climate, cause stability: the initial bump is dampened and no sand wave train is generated. This is clearly related the large wave periods (almost 8 s) that cause strong refraction and a severe reduction in wave angle. Due to this refraction, also the wave height is strongly reduced from, e.g., 2.6 m to 1.47 m.

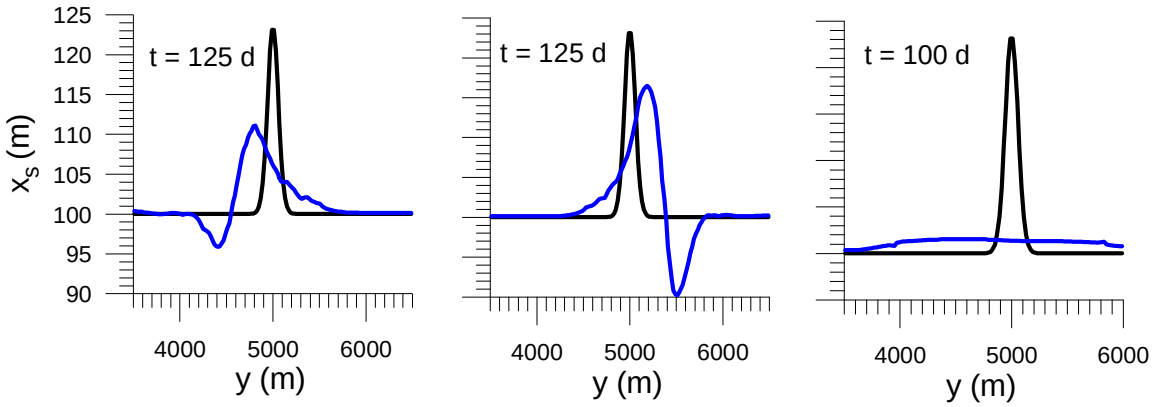

Figure 6. Initial (black) and final (blue) shorelines for tests 1, 2, 3.

5. Tests for the actual wave climate

5.1 1D-morfo model

The linear stability analysis of the shoreline for a wave climate has been applied here following Falqués (2006). For a set of wave conditions (θ_1,H_1,T_1), (θ_2,H_2,T_2) …. (θ_n,H_n,T_n) with relative frequencies p_1, p_2, …, p_n and for each sand wave wavenumber k the complex growth rate σ_i (k) is computed. Then, due to linearity, the actual growthrate for wavenumber k is the average

$$\bar{\sigma} = \sum_{i=1}^{n} p_i \sigma_i \qquad (6)$$

For the full wave climate the shoreline is at the threshold for instability, with a very small real growthrate $\sigma = 3 \cdot 10^{-10}$ s^{-1}, i.e., growth time of about 106 yr. Clearly, if the angles smaller than 40^o are removed from the climate, there is instability with a growth time $\sigma^{-1} = 0.49$ yr and a dominant wavelength of 1100 m (Figure 7). In case of using the full wave climate, the stability or instability is very sensitive to the bathymetric profile used although the growtrates either positive or negative are very small.

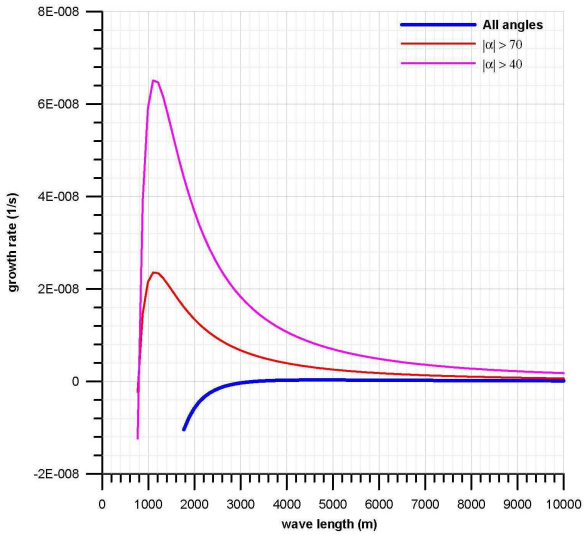

Figure 7. Growthrate (s^{-1}) as a function of wavelength (m) for: i) the actual wave climate (blue), ii) the wave climate without angles below 40^o with shore normal (magenta) and iii) the wave climate without angles below 70^o with shore normal (red) .

5.2 Q2D-morfo model

Running Q2D-morfo with changing wave conditions is still not fully addressed due to numerical instabilities. For example, while the model performs correctly wave transformation for the time series of wave conditions for a full year if bed updating is turned off, when the bed-waves coupling is turned on it crashes after a few weeks. Work is currently under progress to fix it and we hope to be able of presenting more thorough results at the Conference. An interesting test (#4) we have run instead is based on a synthetic time series made from the wave climate. We classified the angles in boxes of 22.5^o and for each box we found the mean H_s and the mean T (see table 2). Then we assigned a number of days to each box according to the probability of occurrence. Of course, the time series can be constructed in many different ways and chronology effects may be here very relevant. We have here gathered the boxes from E-NE to SW by increasing the angle. Different options will be explored and presented at the Conference.

Table 2. Wave conditions for test 4 with Q2D-morfo for the wave climate of Blanes buoy. The angle is with respect to shore normal (positive from the SW)

θ	-85	-70	-47.5	-25	-2.5	20	42.5	65
H_s (m)	0.7	0.82	0.66	0.64	0.5	0.5	0.58	0.57
T_m (s)	4.3	4.7	4.5	4.5	4.2	4.2	4	3.6
Number of days	8	21	10	16	11	11	16	7

Due the numerical instabilities it has been some delay in getting successful experiments and we present here only preliminary results of test 4. It is planned to run for t=1000 d, but results only up to t=50 d are now available because of the paper submission deadline. However, the results are promising. It is found that the shoreline becomes unstable during the E-NE and E waves (θ = -85^o and -70^o) but sand waves start to get damped when the waves come from the

SE (θ = -47.5^o and -25^o). This is seen in Figure 8, through the amplitude of the downdrift embayment that is maximum for t=20 d but has almost disappeared for t=50 d.

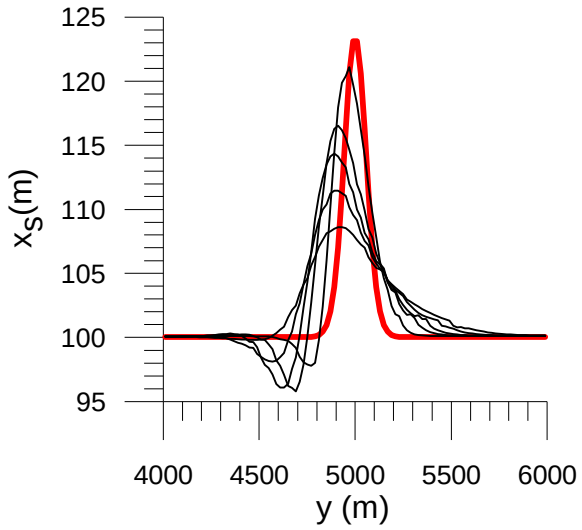

Figure 8. Shoreline evolution for the synthetic time series of wave conditions based on the wave climate (Blanes buoy) and shown in table 2. Initial shoreline in red. The subsequent shorelines are given every 10 d.

6. Discussion and conclusions

Although the study is still in a preliminary stage everything points to the conclusion that Calella beach is at the threshold for high angle wave instability. From the modeling point of view this means that the uncertainty inherent in model parameters like basic cross-shore bathymetric profile or depth of closure may jump from stability to instability or vice versa. Also, the interannual variability in wave climate may also cause that jump. Thus, some time periods may cause slight shoreline instability with the formation of shoreline sand waves that would be damped during other periods. This is consistent with the small amplitude of the sand waves observed along Calella beach. Also, historical images from Google Earth (not shown in the paper) indicate that the sand waves were quite visible during 2002-2009 but less visible during 2010. Interestingly, all computations for unstable conditions, i.e., when the low angle waves are removed from the wave climate, give wavelengths in the range 600-1200 m, which is the range of the observed ones, no matter those simulations are made with Linear Stability Analysis or with nonlinear time evolution. To complete the study, a sensitivity analysis of the linear stability curves of Figure 7 for the wave climate to the bathymetry and the depth of closure should be made. Regarding nonlinear time evolution, the simulation for the wave climate shown in Figure 8 should be completed and the chronology effects should be investigated. Running the model with the actual time series of wave conditions is extremely interesting. Finally, a quantitative analysis of historical shorelines with a principal component analysis (Medellin et al., 2008) should be done and compared to Q2D-morfo outputs for real wave conditions for the corresponding time periods.

Acknowledgements

We gratefully acknowledge the wave data from the XIOM (Xarxa d'Instruments Oceanogràfics I Meteorològics de la Generalitat de Catalunya) and using the Sistema d'Informació Geografica del Litoral de Catalunya, SIGPesca. We appreciate the funding from the Spanish Government through the projects CTM2009-11892 and CTM2012-35398.

References

Ashton, A., A. B. Murray and O. Arnault 2001. Formation of coastline features by large-scale instabilities induced by high-angle waves. *Nature*, 414, 296-300.

Ashton, A., and A. B. Murray 2006a. High-angle wave instability and emergent shoreline shapes: 1. Modeling of sand waves, flying spits, and capes. *Journal of Geophysical Research*, 111, F04011,doi:10.1029/2005JF000422.

Bruun, P. 1954. Migrating sand waves or sand humps, with special reference to investigations carried out on the Danish North Sea Coast, *Proceedings of 5th International Conference on Coastal Engineering*, ASCE, 269-295.

Davidson-Arnott, R. G. D. and A. van Heyningen 2003. Migration and sedimentology of longshore sandwaves, Long Point, Lake Erie, Canada. *Sedimentology*, 50, 1123-1137.

Falqués, A., and D. Calvete 2005. Large scale dynamics of sandy coastlines. Diffusivity and instability. *Journal of Geophysical Research*, 110, C03007, doi:10.1029/2004JC002587.

Falqués, A. 2006. Wave driven alongshore sediment transport and stability of the Dutch coastline. *Coastal Engineering*, 53, 243-254 (2006).

Falqués, A., N. van den Berg, F. Ribas and M. Caballeria 2011a. Modelling shoreline sand waves. Application to the coast of Namibia. *Proceedings of the 7th IAHR Symposium on River, Coastal and Estuarine Morphodynamics*, cd-rom.

Falqués, A., D. Calvete and F. Ribas 2011b. Shoreline Instability due to Very Oblique Wave Incidence: Some Remarks on the Physics. *Journal of Coastal Research*, 27(2), 291-295.

Gravens, M. B. 1999. Periodic shoreline morphology, Fire Island, New York. *Proceedings of Coastal Sediments'99*, ASCE, 1613-1626.

Inman, D. L., M. H. S. Elwany, A. A. Khafagy and A. Golik 1992. Nile Delta Profiles and Migrating Sand Blankets. *Proceedings of 23th International Conference on Coastal Engineering*, ASCE, 269-295.

Kaergaard, K., J. Fredsoe and S. B. Knudsen 2011. Coastline undulations on the West Coast of Denmark: Offshore extent, relation to breaker bars and transported sediment volume. *Coastal Engineering*, 60, 109-122.

Medellín, G., R. Medina, A. Falqués and M. González 2008. Coastline sand waves on a low energy beach at 'El Puntal' spit, Spain. *Marine Geology*, 250, 143-156.

Medellín, G., A. Falqués, R. Medina and M. González 2009. Sand waves on a Low-Energy Beach at 'El Puntal' Spit, Spain: Linear Stability Analysis. *Journal of Geophysical Research*, 114, C03022, doi:10.1029/2007JC004426.

Ruessink, B. G. and M. C. J. L. Jeuken 2002. Dunefoot dynamics along the Dutch coast. *Earth Surface Processes and Landforms*, 27, 1043-1056.

Ryabchuk, D., I. Leontyev, A. Sergeev, E. Nesterova, L. Sukhacheva and V. Zhamoida 2011. The morphology of sand spits and the genesis of longshore sand waves on the coast of the eastern Gulf of Finland. *Baltica* 24 (1), 13–24.

Stive, M. J. F., S. G. J. Aarninkhof, L. Hamm, H. Hanson, M. Larson, K. M. Wijnberg, R. J. Nicholls and M. Capobianco 2002. Variability of shore and shoreline evolution. *Coastal Engineering*, *47*, 211-235

Thevenot M. M. and N. C. Kraus 1995. Longshore sandwaves at Southampton Beach, New York: observations and numerical simulation of their movement. *Marine Geology*, 126, 249-269.

Van den Berg, N., A. Falqués, F. Ribas. 2012a. Modeling large scale shoreline sand waves under oblique wave incidence. *Journal of Geophysical Research*, 117, F03019, doi:10.1029/2011JF002177.

Verhagen, H. J. 1989. Sand waves along the Dutch Coast. *Coastal Engineering*, 13, 129-147.